International Journal of Nanomedicine

Dovepress
open access to scientific and medical research

Open Access Full Text Article

ORIGINAL RESEARCH

Kaempferol-immobilized titanium dioxide promotes formation of new bone: effects of loading methods on bone marrow stromal cell differentiation in vivo and in vitro

This article was published in the following Dove Press journal:
International Journal of Nanomedicine

Shuhei Tsuchiya[1]
Keisuke Sugimoto[2]
Hisanobu Kamio[2]
Kazuto Okabe[1]
Kensuke Kuroda[3]
Masazumi Okido[3]
Hideharu Hibi[2]

[1]Department of Oral and Maxillofacial Surgery, Nagoya University Hospital, Nagoya, Japan; [2]Department of Oral and Maxillofacial Surgery, Nagoya University Graduate School of Medicine, Nagoya, Japan; [3]Institute of Materials and Systems for Sustainability, Nagoya University, Nagoya, Japan

Background: Surface modification of titanium dioxide (TiO_2) implants promotes bone formation and shortens the osseointegration period. Kaempferol is a flavonoid that has the capacity to promote osteogenic differentiation in bone marrow stromal cells. The aim of this study was to promote bone formation around kaempferol immobilized on TiO_2 implants.

Methods: There were four experimental groups. Alkali-treated TiO_2 samples (implants and discs) were used as a control and immersed in Dulbecco's phosphate-buffered saline (DPBS) (Al-Ti). For the coprecipitation sample (Al-cK), the control samples were immersed in DPBS containing 50 µg kaempferol/100% ethanol. For the adsorption sample (Al-aK), 50 µg kaempferol/100% ethanol was dropped onto control samples. The surface topography of the TiO_2 implants was observed by scanning electron microscopy with energy-dispersive X-ray spectroscopy, and a release assay was performed. For in vitro experiments, rat bone marrow stromal cells (rBMSCs) were cultured on each of the TiO_2 samples to analyze cell proliferation, alkaline phosphatase activity, calcium deposition, and osteogenic differentiation. For in vivo experiments, TiO_2 implants placed on rat femur bones were analyzed for bone–implant contact by histological methods.

Results: Kaempferol was detected on the surface of Al-cK and Al-aK. The results of the in vitro study showed that rBMSCs cultured on Al-cK and Al-aK promoted alkaline phosphatase activity, calcium deposition, and osteogenic differentiation. The in vivo histological analysis revealed that Al-cK and Al-aK stimulated new bone formation around implants.

Conclusion: TiO_2 implant-immobilized kaempferol may be an effective tool for bone regeneration around dental implants.

Keywords: kaempferol, titanium implant, surface treatment, biomaterial

Introduction

Titanium dioxide (TiO_2) has been commonly utilized for endosseous implant materials because of its good mechanical properties, chemical resistance, and biocompatibility.[1] In the dental field, its typical use is in dental implants for missing teeth, because such dental implants provide stronger mastication performance than do plate dentures. The principal requirement for this treatment is to bond TiO_2 implants to living bones without the formation of fibrous tissues;[2] this process is termed osseointegration. The treatment term for dental implants is longer than that of other treatments, because several months are needed to obtain proper osseointegration. Thus, a shortened dental implant treatment term would be convenient for patients. Early or even immediate

Correspondence: Shuhei Tsuchiya
Department of Oral and Maxillofacial Surgery, Nagoya University Hospital, 65 Tsuruma-cho, Showa-ku, Nagoya, Aichi 466-8550, Japan
Tel +81 52 744 2348
Fax +81 52 744 2352
Email t-shuhei@med.nagoya-u.ac.jp

submit your manuscript | www.dovepress.com
Dovepress
http://dx.doi.org/10.2147/IJN.S150786

loading requires a higher degree of osseointegration in the early stage of healing.[3] Modifications to the morphology and properties of the implant surface have been examined to obtain stronger and earlier osseointegration, including by control of the surface topography[4] and hydroxyapatite coating.[5] These mechanical and chemical modifications of the TiO_2 surface are already used in clinical treatment. However, these modifications are not enough to shorten the time required for osseointegration. Bioactive molecule (BM) immobilization has recently been applied to TiO_2 implants to obtain stronger and earlier osseointegration.[6] These BMs included recombinant human bone morphogenetic protein-2,[7] type I collagen (ColI),[8] fibronectin,[9] amelogenin,[10] glycan,[11] and arginine–glycine–aspartic acid (RGD) peptide.[12] Furthermore, gene silencing methods were used to relieve inflammation around the TiO_2 implant.[13] Although these BM and genetic engineering methods improved the bone formation surrounding TiO_2 implants, the safety of these methods has not been established; for example, their pharmacodynamics and side effects are unknown. In addition, these methods were too expensive for general use. Furthermore, the effects of these BMs involve only one pathway, such as cell attachment, cell adhesion, or osteogenic induction.

Kaempferol is a typical flavonol-type flavonoid present in a variety of vegetables and fruits. Diets rich in flavonols (a subclass of flavonoids including kaempferol and quercetin) have been positively associated with better skeletal health in humans.[14,15] Previous reports have shown that kaempferol has osteogenic properties.[16–20] Kaempferol reduced osteoclastic bone resorption by inhibiting the receptor activator of nuclear factor-κB (NF-κB) (RANK) protein and activating caspases.[21] Kaempferol inhibited tumor necrosis factor-α (TNF-α)-induced production of IL-6 and monocyte chemoattractant protein-1 (MCP-1) in MC3T3-E1 osteoblast-like cells, and only kaempferol blocked TNF-α-induced translocation of NF-κB subunit p65 from the cytoplasm to the nucleus.[22] Kaempferol also increased alkaline phosphatase (ALPase) activity in MG-63 osteoblast-like cells through the extracellular regulated kinase (ERK) and estrogen receptor pathways.[23] These results indicate that kaempferol is a potent anti-osteoclastic agent owing to its action on both osteoclasts and osteoblasts. In addition, kaempferol promoted the expression of osteogenic gene expression in osteoblasts in vitro[16,18–20] and new bone formation in vivo.[16,17] Notably, kaempferol promoted osteogenic effects in an ovariectomized animal model.[17,24] Moreover, kaempferol has shown anti-inflammatory function,[25] anti-oxidant activity,[26] and anti-microbial activity;[27] these effects are known to promote bone healing.[28,29]

Bone-like mineral coatings are commonly applied to titanium implants in orthopedic and dental applications to enhance bone–TiO_2 contact.[30] These bone-like coatings have been shown to control the release of BMs.[31] There are many methods for loading BMs with biomimetically formed minerals, such as physical adsorption, covalent binding, and biomimetic coprecipitation, each of which results in different loading efficiencies and release kinetics.[32] BMs in bone-like minerals are released slowly because of the slow degradation characteristic of mineral coatings in physiological conditions.[10]

In this study, we hypothesize that TiO_2 implants loaded with kaempferol promote bone formation. Two methods of loading kaempferol on TiO_2 were used. The first was the adsorption method, which simply loaded kaempferol on to the TiO_2. The second was coprecipitation, which precipitated the bone-like mineral coating by immersing an alkali-treated TiO_2 substrate in Dulbecco's phosphate-buffered saline (DPBS) containing $CaCl_2$.[33] The different release profiles of these methods influenced bone formation on the surface of TiO_2 in vitro and in vivo.

Materials and methods

Animals

Six-week-old female Sprague–Dawley rats (n=15, weighing 200–230 g) were purchased from Japan SLC (Hamamatsu, Japan). All the animal experiments were conducted in compliance with the protocols of the Regulations on Animal Experiments in Nagoya University which was approved by the Nagoya University Animal Experiment Committee (permit number #28487, approval November 11, 2016). Animals were housed in a temperature-controlled room with a 12/12 h alternating light–dark cycle and were allowed free access to water and food throughout the day.

Cultivation of rat bone marrow stromal cells (rBMSCs)

rBMSCs were harvested from rat femurs and cultured in Dulbecco's Modified Eagle's Medium with fetal bovine serum, glutamine, and penicillin–streptomycin (Kohjin Bio Co., Saitama, Japan) under standard cell culture conditions (a sterile, 37°C, humidified, 5% CO_2 environment). rBMSCs at the fifth passage were used for all cell culture experiments. The growth medium was changed every 3 days until the cells reached 80%–100% confluence.

Preparation of kaempferol-loaded TiO_2 implant screws and discs

Commercially pure TiO_2 discs (grade IV; Ofa, Tokyo, Japan) with diameters of 10 mm and thicknesses of 1 mm were used.

The screw-type implants (Ofa) used in this study were of the same design (4 mm long and 2 mm in diameter) as those described in previous reports.[34]

These TiO_2 substrates were washed by ultrasonic cleaning in pure acetone, ethanol, and distilled water for 15 min each, and were then dried at 40°C. The TiO_2 substrates were then soaked in 5 mL of 1 M sodium hydroxide (NaOH) aqueous solution at 140°C for 6 h, washed gently with Milli-Q® water (Merck Millipore, Darmstadt, Germany), and dried at 40°C. These treated TiO_2 substrates are denoted "alkali-treated Ti".

The two loading procedures of kaempferol, adsorption and coprecipitation, were used according to previously reported methods.[32] The vehicle sample (control) TiO_2 screws and discs were not treated. Alkali-treated TiO_2 samples were used as controls and immersed in 1 mL of DPBS for 24 h at 37°C (Al-Ti). To prepare the coprecipitation sample (Al-cK), control samples were immersed in 1 mL of DPBS containing 50 µg kaempferol/100% ethanol for 24 h at 37°C. To prepare the adsorption sample (Al-aK), 100 µL of 100% ethanol containing 50 µg kaempferol was dropped on to control samples and dried in air. All solutions were sterilized by filtration using a membrane with a pore size of 0.22 µm before use. The preparation methods are summarized in Figure 1.

Scanning electron microscopy

The morphological surface characteristics of the TiO_2 samples were observed with a thermal field scanning electron microscope (JSM-7610F; JEOL Ltd., Tokyo, Japan) at an accelerating voltage of 20 kV. Electron-dispersive spectroscopy (EDS) analysis was also carried out after the treatment to evaluate the TiO_2 surface chemical composition. Backscatter images were taken for analysis of elemental compositional differences across the surfaces.

Kaempferol release assay

Drug release from the drug-loaded TiO_2 discs was investigated by immersing them in 30 mL of Hanks' solution. The amount of drug released was measured using ultraviolet–visible (UV-vis) spectroscopy (V-650 spectrometer; JASCO, Tokyo, Japan). Release readings were taken at 0, 2, 6, 12, 24, 72, and 168 h. Released drug concentration was calculated based on the calibration curve obtained for the drug; the corresponding absorbance was measured at 366 nm. Finally, the drug release profiles were plotted with release percentage versus time for each experimental set with regard to burst and delayed releases. The release percentage (weight percentage) was calculated from the amount of drug released into the Hanks' solution divided by the total amount of drug

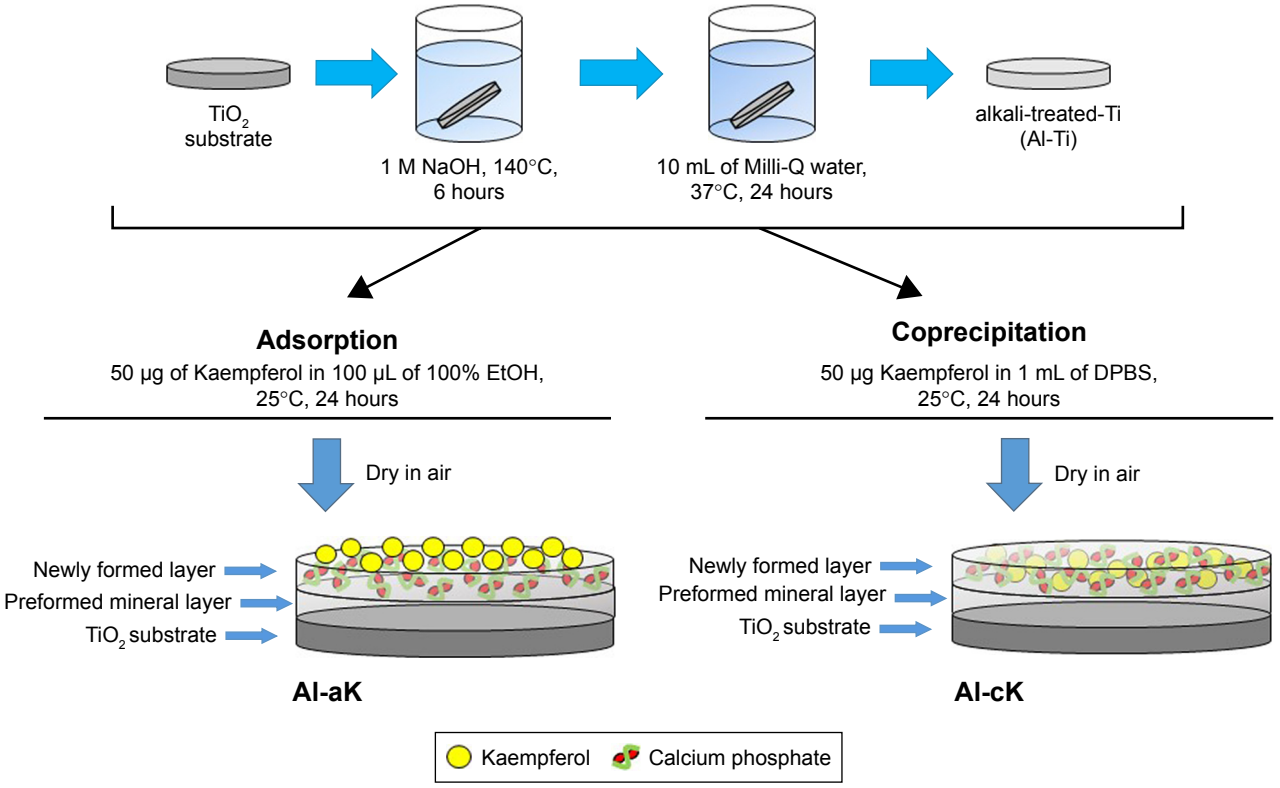

Figure 1 Sketch map of the loading of bioactive molecules on alkali-treated TiO_2.
Abbreviations: TiO_2, titanium dioxide; EtOH, ethanol; DPBS, Dulbecco's phosphate-buffered saline; Al-aK, alkali-treated adsorption with kaempferol; Al-cK, alkali-treated coprecipitation with kaempferol.

(weight) released after 168 h as determined by UV-vis spectrophotometry and multiplied by 100.[35]

Measurement of cell proliferation

rBMSCs were plated at a density of 5×10^3 cells/mL on the four samples of TiO_2 discs. rBMSCs in each well were counted using the WST-8 kit (Cell counting Kit-8; Dojindo Laboratories, Kumamoto, Japan). The counting technique employed a tetrazolium salt that produces a highly water-soluble formazan dye. After 1 h incubation with the reagent according to the manufacturer's instructions, the relative cell number was determined by measuring the absorbance of light at a wavelength of 450 nm on days 1, 3, and 7 (Model 650 Microplate Reader; Bio-Rad Laboratories, Hercules, CA, USA).

Assay for ALPase activity

rBMSCs were plated at a density of 5×10^3 cells/mL on the four samples of TiO_2 discs. For quantitative analysis of ALPase activity, p-nitrophenol production was measured at 37°C for 6 min in Milli-Q water using a SIMGAFAST p-Nitrophenyl phosphate Tablet set (Sigma-Aldrich, St. Louis, MO, USA) as a substrate. The relative amount of p-nitrophenol was estimated from the light absorbance at 405 nm on days 1, 3, and 7 (Bio-Rad Laboratories).

Analysis of gene expression in rBMSCs

The rBMSCs were seeded at a density of 1.0×10^6 cells on the four experimental groups of TiO_2 discs and were cultured for 1, 3, and 7 days. Total RNA was extracted with TRIzol reagent (Thermo Fisher Scientific, Waltham, MA, USA) according to the manufacturer's protocol. cDNA was synthesized from 1 µg total RNA in a 20 µL reaction containing 10× reaction buffer, 5 mM deoxynucleoside triphosphate (dNTP) mixture, 1 U/µL RNase inhibitor, 0.25 U/µL reverse transcriptase (M-MLV reverse transcriptase; Invitrogen), and 0.125 µM random primers (Takara, Tokyo, Japan). Real-time polymerase chain reaction (PCR) was performed to quantify absolute mRNA expression using an ABI PRISM 7900HT system (Thermo Fisher Scientific) with Absolute QPCR SYBR Green Mixes (Applied Biosystems). Primer sequences are listed in Table 1. The thermocycling parameters were optimized at 50°C for 2 min, 95°C for 15 min, 40 cycles of 95°C for 15 s, and 61°C for 1 min. Cycle threshold (Ct) values were determined and used to calculate relative gene amounts. PCR products were quantified and the amplification of the target genes listed in Table 1 was compared with that of the reference gene *glyceraldehyde-3-phosphate dehydrogenase* (*GAPDH*), with calibrator normalization and amplification efficiency correction.

Table 1 Sequences of primer pairs used in RT-PCR

Gene	Sequence	Accession number of reference
Runx2	Forward 5′-CACAAGTGCGGTG CAAACTT Reverse 5′-CACTGACTCGGTTG GTCTCG	NM_053470.2
Osteopontin	Forward 5′-ACAGTATCCCGATG CCACAG Reverse 5′-GACCACGAGGTTGG GATGAC	XM_002728077
ALP	Forward 5′-TCCTTAGGGCCACC GCTC Reverse 5′-GGGCAGTGTCAGCC GTTAAT	NM_013059
Osteocalcin	Forward 5′-ATTGTGACGAGCTA GCGGAC Reverse 5′-TCGAGTCCTGGAGA GTAGCC	M25490
Collagen type I	Forward 5′-TGACGCATGGCCAA GAAGAC Reverse 5′-CAGGTTTCCACGTC TCACCAT	NM_053304.1
Osteonectin	Forward 5′-TCAGACGGAAGC TGCAGAA Reverse 5′-TTTTCAGCCACCAC CTCCTC	Y13714
GAPDH	Forward 5′-CAGGAAATGATGACC TCCTGAAC Reverse 5′-TGTTTTTGTAAGTATCT TGGTGCCT	AF106860

Abbreviations: RT-PCR, reverse transcription polymerase chain reaction; Runx2, runt-related transcription factor 2; ALP, alkaline phosphatase; GAPDH, glyceraldehyde-3-phosphate dehydrogenase.

Analysis of calcium deposition in vitro

Calcified nodules on the cells were demonstrated using an assay based on Alizarin Red S staining. rBMSCs were plated at a density of 5×10^3 cells/mL on the four samples of TiO_2 discs and cultured for 1, 7, and 14 days. Quantification of staining was carried out as described by Gregory et al.[36] In brief, 800 µL of 10% (v/v) acetic acid was added to each well, and the plate was incubated at room temperature for 30 min with shaking. The monolayer was then scraped from the plate and transferred with 10% (v/v) acetic acid. The slurry was heated to exactly 85°C for 10 min. The slurry was then centrifuged at 20,000 *g* for 15 min and 500 µL of the supernatant was removed. Then, 200 µL of 10% (v/v) ammonium hydroxide was added to neutralize the acid. Aliquots (150 µL) of the supernatant were read in triplicate at

405 nm in a 96-well format using opaque-walled, transparent-bottomed plates.

Surgical procedure of implantation

The TiO_2 screws were inserted into the femurs as previously described.[37] The rats were anesthetized with a combination of inhaled diethyl ether vapor (3 mL/chamber) and an intraperitoneal injection of pentobarbital (20 mg/kg). A 10 mm incision was made on the skin over the distal femur, and the bone was exposed. A unicortical implant floor was created 7 mm from the distal end of the bone using a dental round bar (1.5 mm diameter) at a rotation speed of 1,500 rpm or less. The control, Al-Ti, Al-cK, and Al-aK implants were inserted into the cortical bone. The soft tissues were then returned to their normal positions and sutured with 3-0 Vicryl® SH-1 (Ethicon, Tokyo, Japan).

Histological processing and bone–implant contact (BIC) rate (%) measurements

Two to four weeks after implantation, the rats (n=5 each) were killed while under deep anesthesia, and the femoral screws were excised. The samples were embedded in Technovit 7100® (Okenshoji Co., Tokyo, Japan). Each block was cut along the long axis of the screw into 50-µm-thick sections and polished samples were stained with 1% toluidine blue for 15 min and embedded in Malinol 750 cps (MUTO PURE CHEMICALS CO., LTD, Tokyo, Japan). Microscopic images of the sections were displayed on a monitor, and the BIC was measured by inputting the image data into a computer and analyzing them with image-analysis software (VMS-50 VideoPro®; Inotech Corporation, Hiroshima, Japan). The BIC rate was calculated using the following equation: Bone contact rate (%) = Direct implant–bone contact/Peri-implant length.

Statistical analysis

Analysis of variance (ANOVA) was performed on data sets when appropriate using a significance of p-values <0.05. Separate one-way analyses of variances were used to analyze the release assay, cell attachment, cell proliferation, ALPase activity, calcium deposition, and BIC rate measurements. The Student–Newman–Keuls post hoc comparison test was used for pairwise comparisons.

Results

Effects of loading methods on surface characteristics

Non-treated TiO_2 screws showed the typical topography of machined, polished TiO_2 (Figure 2A). A non-uniform, rugged layer was apparent on the surface of the Al-Ti (Figure 2B). Small and large microspheres were apparent on the surface of Al-cK and Al-aK (Figure 2C and D). Microsphere morphology was the same in Al-cK and Al-aK. EDS analysis showed that the components on the surfaces of Al-Ti, AL-aK, and Al-cK were Ti, calcium, phosphate, and carbon (Figure 3A–D). The amount of Ti on the surface of Al-aK was significantly lower than that on the control, Al-Ti, and Al-cK. The amount of Ti on the surface of Al-aK was also significantly lower than that on the control and Al-Ti (Figure 3E). The amount of carbon on the surface of Al-aK was significantly higher than that on Al-cK. The amount of carbon on the surface of Al-Ti was infinitesimal (Figure 3F). The amount of phosphate on the surface of Al-cK was significantly higher than that on Al-Ti and Al-aK; however, there were no significant differences between Al-Ti and Al-aK (Figure 3G). The amount of calcium on the surface of Al-cK was significantly higher than that on Al-Ti; again, there were no significant differences between Al-Ti and Al-cK (Figure 3H).

The difference in kaempferol immobilization method did not affect surface topology. EDS analysis revealed kaempferol immobilized on the TiO_2 surface, because kaempferol contains carbon atoms and DPBS does not. EDS analysis also showed that kaempferol and calcium phosphate covered the surfaces of Al-aK and Al-cK. Furthermore, the amount of kaempferol on Al-aK was significantly larger than that on Al-cK.

In vitro drug release of kaempferol

Drug-release profiles of kaempferol-loaded TiO_2 discs over 168 h are presented in Figure 4. The release efficiency (percentage of drug released) at various time intervals is shown. The drug-release kinetics proceeded through two phases. In the first phase (6 h), about 14% of kaempferol on Al-cK was released rapidly. About 5% of kaempferol on Al-aK was released gradually. In the second phase (12–168 h), about 88% of kaempferol on Al-aK was burst released; this released quantity was significantly higher than the quantities released in the other experimental groups. The second phase of release for Al-cK was a gradual release of about 37%.

Effects of kaempferol on cell attachment and proliferation

The analysis of cell proliferation in the four experimental groups showed no significant differences at 1 day and 3 days of cultivation (Figure 5). After 7 days of cultivation, the cell number on Al-aK was significantly higher than that on Al-Ti and Al-cK, but not significantly higher than that on

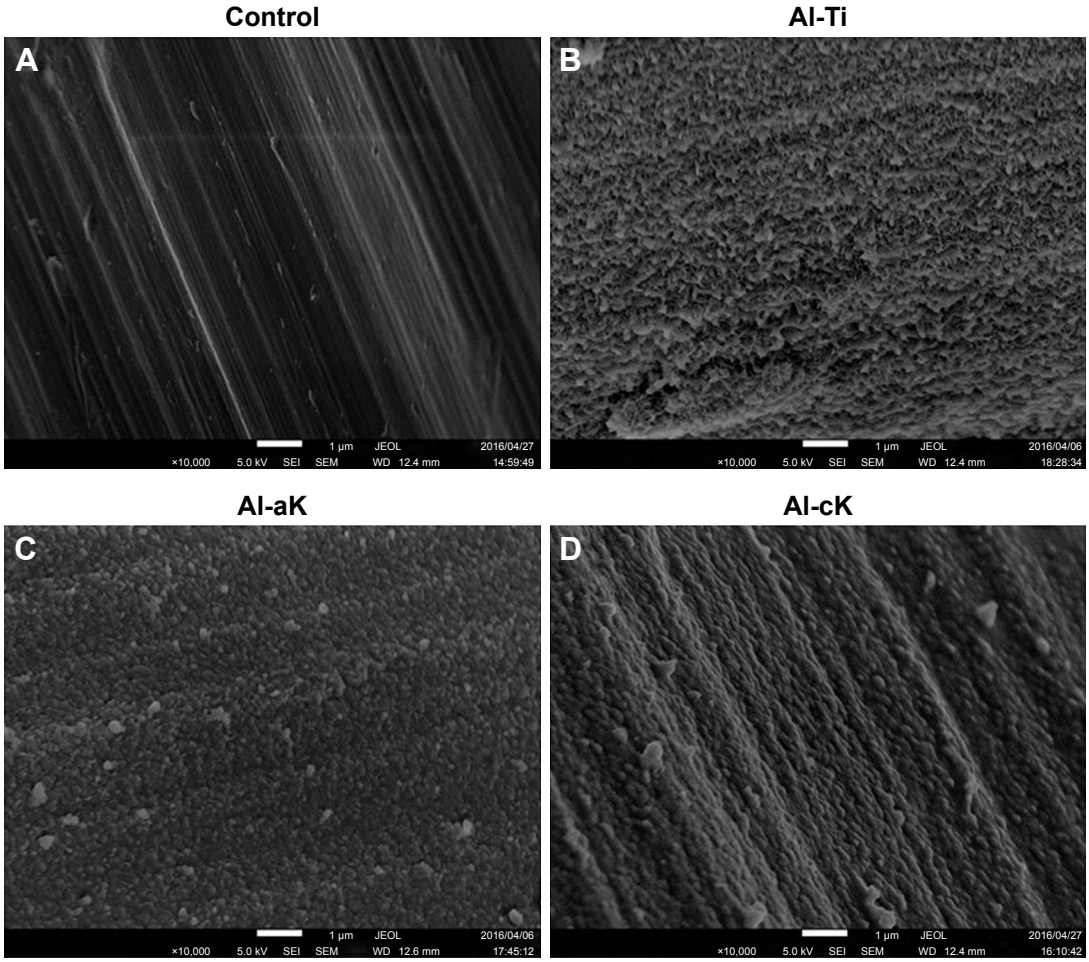

Figure 2 SEM micrograph of the implant surface. (**A**) Control TiO_2 surface showing typical machined surface topology. (**B**) After alkali treatment, the surface of Al-Ti shows fine nanometric topology. (**C**) After alkali treatment and adsorption of kaempferol, the surface of Al-aK shows round-shaped structures. (**D**) After alkali treatment and co-precipitation of kaempferol, the surface of Al-cK shows round-shaped structures.
Note: Magnification: 10,000×.
Abbreviations: SEM, scanning electron microscopy; TiO_2, titanium dioxide; Al-Ti, alkali-treated TiO_2; Al-aK, alkali-treated adsorption with kaempferol; Al-cK, alkali-treated coprecipitation with kaempferol; JEOL, JEOL Ltd.; SEI, secondary electron image; WD, working distance.

the control. There were no significant differences among the control, Al-Ti, and Al-cK.

Effects of kaempferol on ALPase activity

ALPase activity of rBMSCs cultured in the four experimental groups showed no significant differences at 1 and 3 days of cultivation. After 7 days of cultivation, ALPase activities of rBMSCs cultured on Al-aK and Al-cK were significantly higher than those on the control and Al-Ti (Figure 6). However, there were no significant differences between ALPase activities of rBMSCs cultured on Al-aK and Al-cK.

Effects of kaempferol on calcium deposition

After 7 days of cultivation, the calcium deposition of rBMSCs cultured on Al-aK was significantly higher than that on the control, Al-Ti, and Al-cK. The calcium deposition of rBMSCs cultured on Al-cK was significantly higher than that on Al-Ti and the control, but significantly lower than the calcium deposition on Al-aK. After 14 days of cultivation, the calcium deposition of rBMSCs cultured on Al-aK and Al-cK was significantly higher than that on the control and Al-Ti. There were no significant differences between the control and Al-Ti at any time point (Figure 7).

Effects of kaempferol on gene expression in rBMSCs

Results obtained from real-time reverse transcription polymerase chain reaction (RT-PCR) showed that *Runx2* (*runt-related transcription factor 2*) and *ALP* (*alkaline phosphatase*) were up-regulated in rBMSCs grown on Al-Ti, Al-aK, and Al-cK after 1 day of cultivation (Figure 8A). After 3 days of cultivation, the mRNA expressions of *osteocalcin* (*OCN*), *osteonectin* (*ON*), *osteopontin* (*OPN*), and *ALP* in rBMSCs

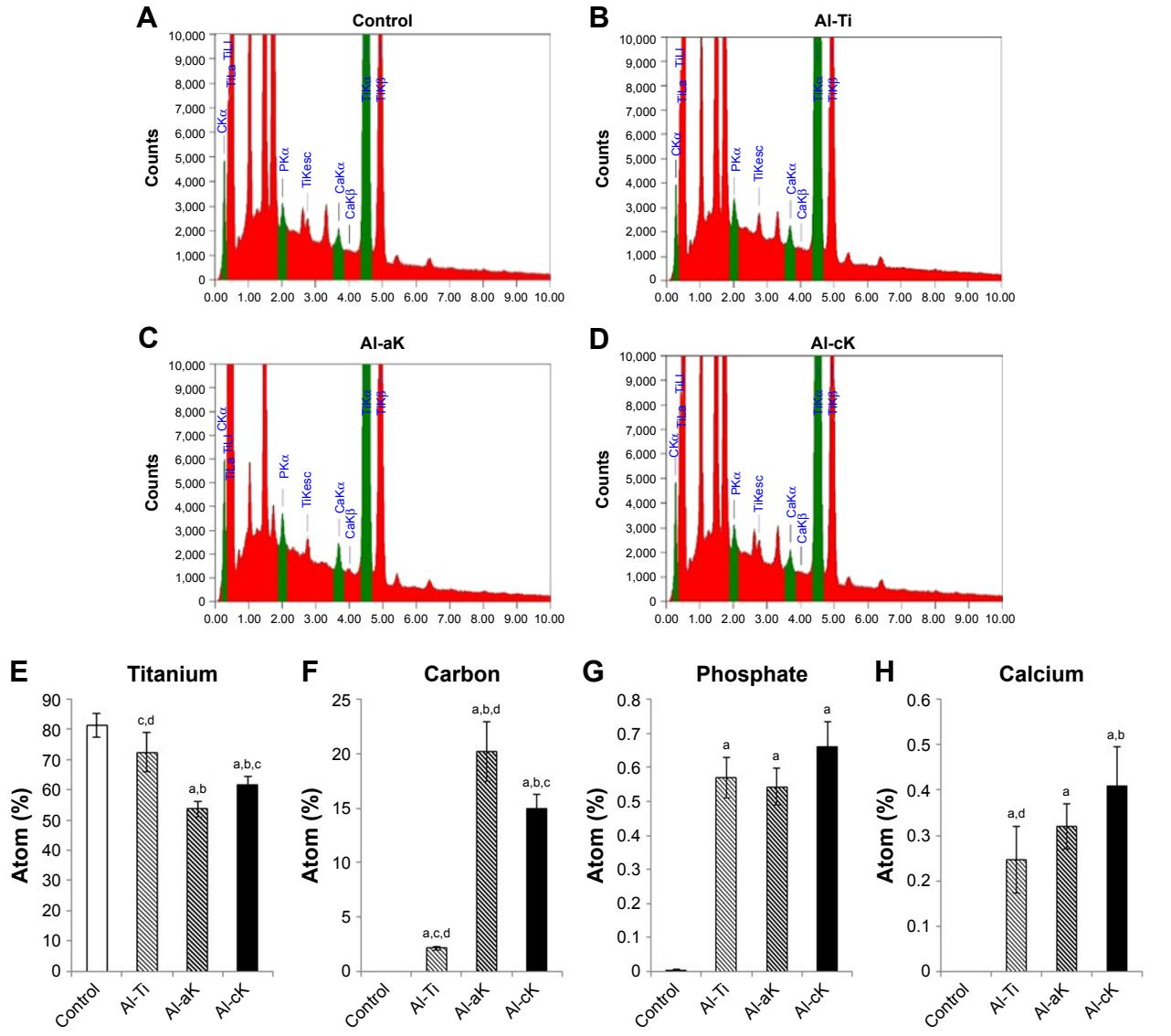

Figure 3 Characterization of TiO_2 surface using EDS analysis. EDS spectrum of (**A**) control, (**B**) Al-Ti, (**C**) Al-aK, and (**D**) Al-cK showing each metallic element on the TiO_2 surface. Quantification of individual metallic elements shows (**E**) titanium, (**F**) carbon, (**G**) phosphate, and (**H**) calcium.

Notes: Data are expressed as means (n=3) with error bars representing standard deviations; [a]$p<0.05$ compared to control; [b]$p<0.05$ compared to Al-Ti; [c]$p<0.05$ compared to Al-aK; [d]$p<0.05$ compared to Al-cK.

Abbreviations: EDS, electron-dispersive spectroscopy; TiO_2, titanium dioxide; Al-Ti, alkali-treated TiO_2; Al-aK, alkali-treated adsorption with kaempferol; Al-cK, alkali-treated coprecipitation with kaempferol; CKα, carbon Kα; TiLl, titanium Ll; PKα, phosphate Kα; TiKesc, titanium Kesc; CaKα, calcium Kα; CaKβ, calcium Kβ; TiKα, titanium Kα; TiKβ, titanium Kβ.

grown on Al-aK and Al-cK were approximately two-fold higher than those on the control and Al-Ti (Figure 8B). After 7 days of cultivation, the mRNA expressions of *Runx2*, *OCN*, *ON*, *OPN*, and *ALP* in rBMSCs grown on Al-aK and Al-cK were approximately two- to four-fold higher than those on the control and Al-Ti (Figure 8C); in addition, mRNA expressions of *Runx2*, *ON*, and *OPN* in rBMSCs grown on Al-aK were higher than those on Al-cK.

Measurement of BIC rate

Histological detection showed that all implants remained in the tibias at the initial operating position, and there were no signs of loosening or dislocation; this demonstrated that the implants were able to connect to the bones well under all circumstances (Figure 9). No adverse effects (such as osteonecrosis or inflammatory responses) were observed in the clinical inspection and histological figures at 4 weeks after implantation. Quantitative analysis revealed that the BICs (%) of Al-aK and Al-cK were significantly higher than those of the control and Al-Ti at 2 and 4 weeks after implantation. The BIC (%) of Al-Ti was significantly higher than that of the control at 4 weeks after implantation.

Discussion

The surfaces of TiO_2 implants have been modified in various ways to improve rigid and early fixation. Kaempferol is a

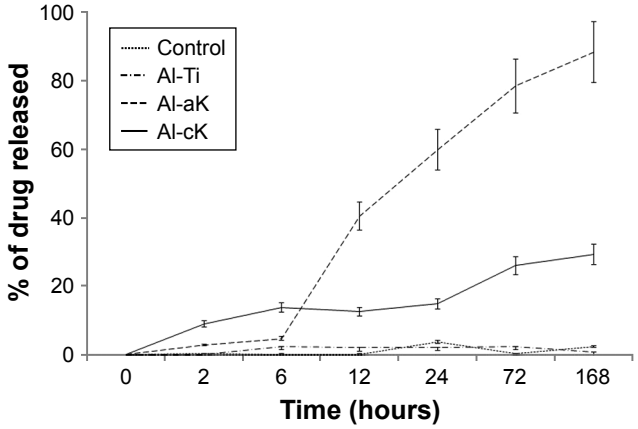

Figure 4 Drug-release graph of kaempferol from TiO_2 discs in Hanks' solution for 168 h.
Note: Data are expressed as means (n=5) with error bars representing standard deviations.
Abbreviations: TiO_2, titanium dioxide; Al-Ti, alkali-treated TiO_2; Al-aK, alkali-treated adsorption with kaempferol; Al-cK, alkali-treated coprecipitation with kaempferol; h, hours.

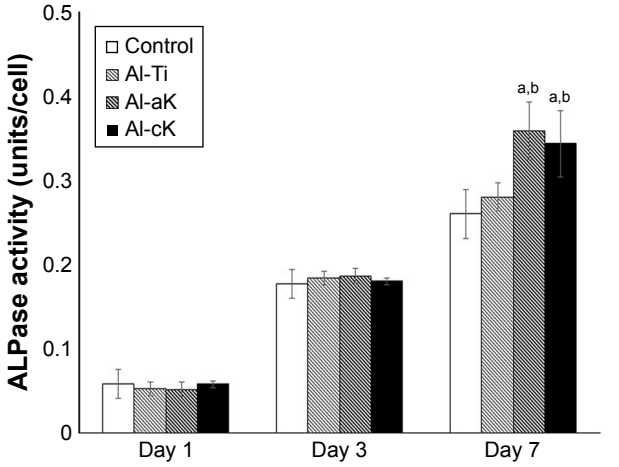

Figure 6 Normalized ALPase activity with respect to total protein of rBMSCs cultured on the representative experimental groups for 1, 3, and 7 days.
Notes: Data are expressed as means (n=3) with error bars representing standard deviations; [a]$p<0.05$ compared to control; [b]$p<0.05$ compared to Al-Ti.
Abbreviations: ALPase, alkaline phosphatase; rBMSC, rat bone marrow stromal cell; TiO_2, titanium dioxide; Al-Ti, alkali-treated TiO_2; Al-aK, alkali-treated adsorption with kaempferol; Al-cK, alkali-treated coprecipitation with kaempferol.

flavonoid that accelerates osteogenic differentiation in bone marrow stromal cells (BMSCs).[18] The present study was the first trial to examine the effect of kaempferol application to the surface of TiO_2 implants.

The difference in kaempferol immobilization method did not affect surface topology. In a previous report, coprecipitation of minerals and osteogenic growth peptide (OGP) on TiO_2 resulted in mineral crystallites larger than those formed by the adsorption method.[32] It has been suggested that the differences depend on the drug immobilized on TiO_2. Kaempferol affects the osteogenic properties of BMSCs, but does not affect mineralization itself. EDS analysis revealed kaempferol immobilized on the TiO_2 surface, because kaempferol contains carbon atoms and DPBS does not. EDS analysis also showed that kaempferol and calcium phosphate covered the surfaces of Al-aK and Al-cK. Furthermore, the amount of kaempferol on Al-aK was significantly larger than that on Al-cK. However, these measurements have no bearing on the amount of kaempferol contained in the

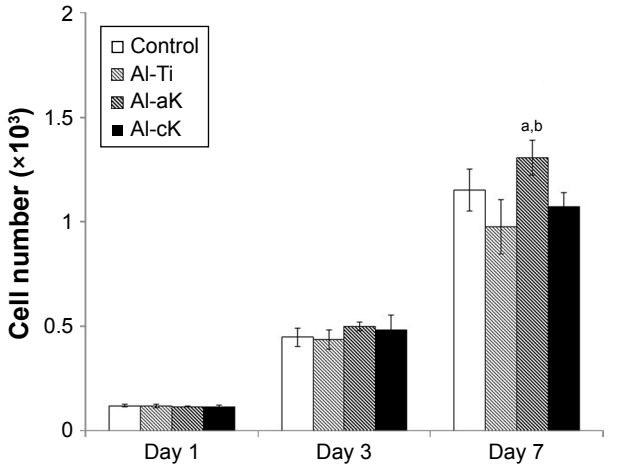

Figure 5 Cell proliferation of rBMSCs adhered to the representative samples in growth medium for 1, 3, and 7 days.
Notes: Data are expressed as means (n=3) with error bars representing standard deviations; [a]$p<0.05$ compared to Al-Ti; [b]$p<0.05$ compared to Al-cK.
Abbreviations: rBMSC, rat bone marrow stromal cell; TiO_2, titanium dioxide; Al-Ti, alkali-treated TiO_2; Al-aK, alkali-treated adsorption with kaempferol; Al-cK, alkali-treated coprecipitation with kaempferol.

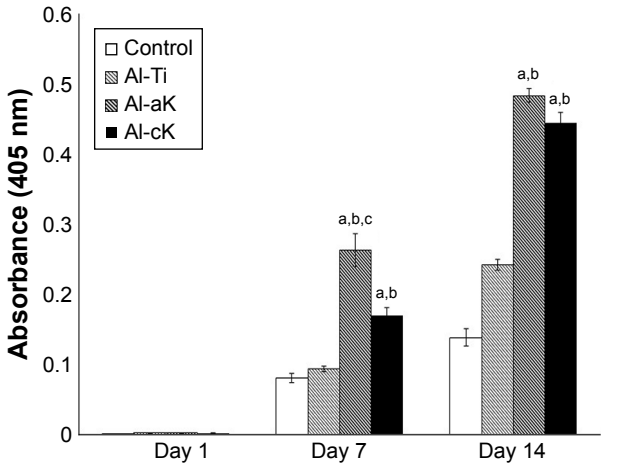

Figure 7 Calcium deposition of rBMSCs cultured on the representative experimental groups for 1, 7, and 14 days. Calcium deposition quantification using the Alizarin Red S assay.
Notes: Data are expressed as means (n=3) with error bars representing standard deviations; [a]$p<0.05$ compared to control; [b]$p<0.05$ compared to Al-Ti; [c]$p<0.05$ compared to Al-cK.
Abbreviations: rBMSC, rat bone marrow stromal cell; Al-Ti, alkali-treated TiO_2; Al-aK, alkali-treated adsorption with kaempferol; Al-cK, alkali-treated coprecipitation with kaempferol; TiO_2, titanium dioxide.

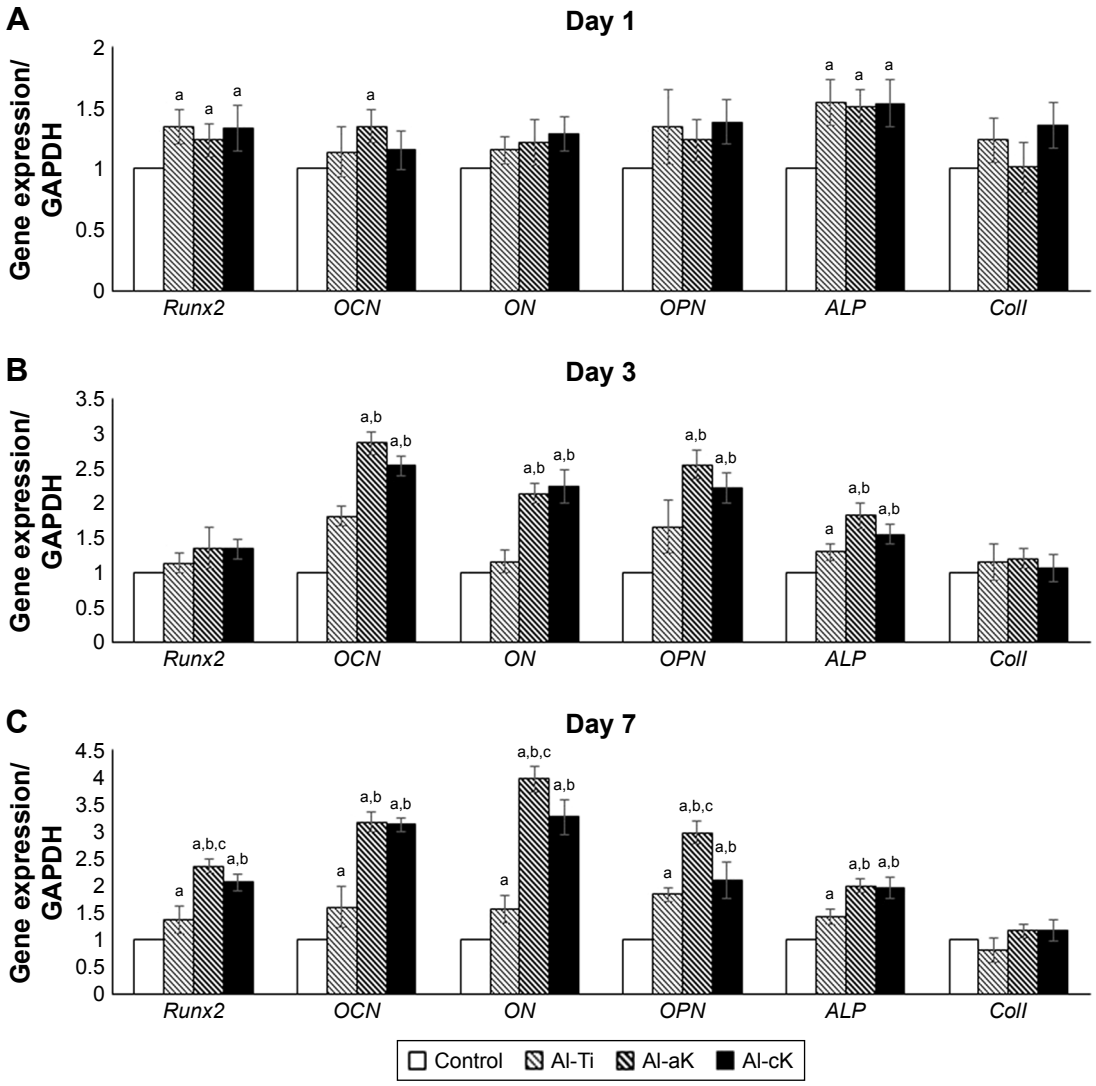

Figure 8 Gene expression of rBMSCs cultured on the representative experimental groups for (**A**) 1, (**B**) 3, and (**C**) 7 days.
Notes: Data are expressed as means (n=3) with error bars representing standard deviations; [a]$p<0.05$ compared to control; [b]$p<0.05$ compared to Al-Ti; [c]$p<0.05$ compared to Al-cK.
Abbreviations: rBMSC, rat bone marrow stromal cell; Al-Ti, alkali-treated TiO_2; Al-aK, alkali-treated adsorption with kaempferol; Al-cK, alkali-treated coprecipitation with kaempferol; TiO_2, titanium dioxide; GAPDH, glyceraldehyde-3-phosphate dehydrogenase; *Runx2*, *runt-related transcription factor-2*; *OCN*, *osteocalcin*; *ON*, *osteonectin*; *OPN*, *osteopontin*; *ALP*, *alkaline phosphatase*; *Coll*, *type I collagen*.

samples, as EDS only analyzed atomics qualitatively on the surface of the samples.

These results are consistent with those of a previous report at long-term time points after 6 h.[32] The release pattern of kaempferol from the mineral layer of Al-cK was suggested to mainly depend on the dissolution of the mineral layer and the diffusion of kaempferol in the mineral layer.[38] A previous report showed that the mineral layer was composed of two sublayers: a top layer composed of loose calcium phosphate crystals and a bottom layer composed of dense apatite crystal.[39] The top calcium phosphate layer can gradually dissolve under physiological conditions,[40] while the bottom apatite layer hardly degrades.[41]

The results of the present study suggest that kaempferol released from Al-cK during the first 6 h was contained in the top layer and kaempferol released after 6 h was contained in the bottom layer. However, drug release from Al-cK was gradual in our study, which is inconsistent with the results of a previous study.[32] This discrepancy is due to the differences in water solubility of OGP and kaempferol. OGP is soluble in water, but kaempferol is hydrophobic.

We hypothesized that different release and existence profiles of kaempferol would influence the osteogenic differentiation in BMSCs, because kaempferol stimulates osteogenic differentiation in a dose-dependent way, and the system of drug delivery affects the cell activity.[42] In a

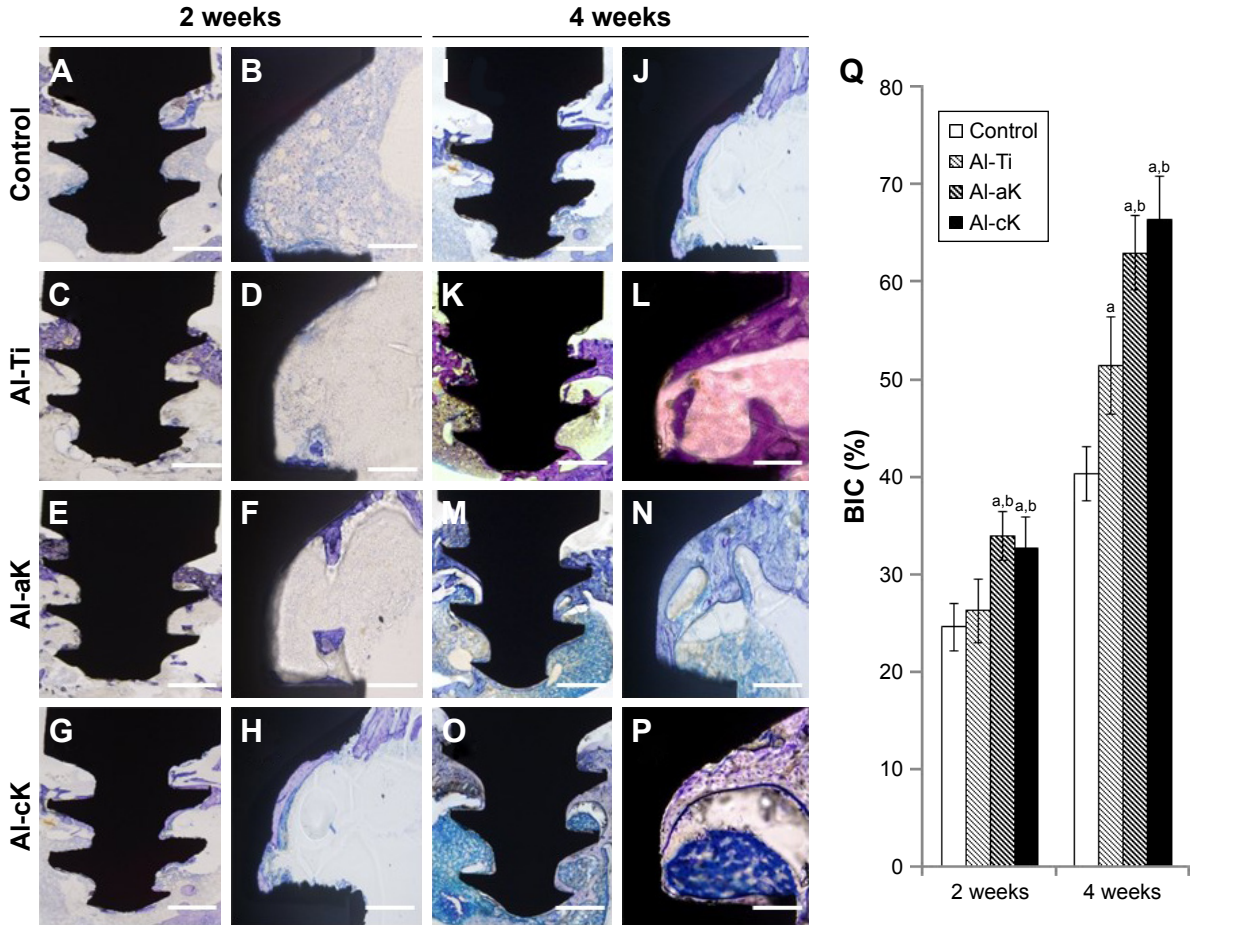

Figure 9 Histological analysis around the TiO_2 implants in vivo. Bone morphogenesis around TiO_2 implants as observed under 100× magnification at 2 weeks after implantation (**A**–**H**) and 4 weeks after implantation (**I**–**P**). (**A**, **B**, **I**, **J**) Control; (**C**, **D**, **K**, **L**) Al-Ti implants; (**E**, **F**, **M**, **N**) Al-aK implants; and (**G**, **H**, **O**, **P**) Al-cK implants. Bars indicate 500 μm (**A**, **C**, **E**, **G**, **I**, **K**, **M**, **O**) and 100 μm (**B**, **D**, **F**, **H**, **J**, **L**, **N**, **P**). (**Q**) Average histomorphometric values of BIC.
Notes: Data are expressed as means (n=3) with error bars representing standard deviations; $^{a}p<0.05$ compared to control; $^{b}p<0.05$ compared to Al-Ti.
Abbreviations: TiO_2, titanium dioxide; Al-Ti, alkali-treated TiO_2; Al-aK, alkali-treated adsorption with kaempferol; Al-cK, alkali-treated coprecipitation with kaempferol; BIC, bone–implant contact.

previous study, an OGP-coprecipitation method promoted osteogenic differentiation using gene expression analysis in BMSCs compared with an OGP-adsorption method.[32] In this study, kaempferol affected the ALPase activity, but the loading method did not. This was consistent with previous reports. In addition, the cell proliferation was affected by the addition and loading method of kaempferol. Kaempferol also inhibited cell proliferation of cancer cells.[43] The measurement of cell proliferation assay in this study also contradicted previous studies. These results indicated that the differences depended on the loading method of kaempferol. The effect on proliferation in this previous study may be different from that of the Al-aK and Al-cK methods in this study. The calcium deposition and gene expression of rBMSCs were also affected by the loading method of kaempferol, and corresponded with the drug-release assay results. These results suggested that differentiation of rBMSCs was caused not by kaempferol on the surface of TiO_2, but by released kaempferol. The stimulation rate of *Runx2* expression was slower than that of a previous study.[16] This result indicated that the differences depended on the cell differentiation stage. *OCN*, *ON*, and *OPN* are extracellular matrix (ECM) proteins of bone tissue, and their expression plays an important role in mineralization by binding to collagen fiber and calcium.[44] These BMSC-derived ECM proteins affected the calcium deposition instead of *ColI*. The expression patterns in rBMSCs from all experimental groups corresponded to the calcium deposition results. The gene expression of *ALP* in rBMSCs cultured on Al-aK and Al-cK was also stimulated. A previous study has also shown that kaempferol has a stimulatory effect on *ALP* activity through the ERK pathway.[23] Furthermore, *ColI* expression in MC3T3-E1 cells has also been shown to be stimulated by kaempferol.[6] Kaempferol released from a titanium surface produced the same effect in rBMSCs as kaempferol added into the medium. This result indicated that the differences observed may depend on the

characteristics of the cell type. Taken together, the in vitro results indicated that Al-aK provides the best cell responses in terms of cell proliferation, *ALP* activity, calcium deposition, and osteogenic differentiation.

In the in vivo study, kaempferol promoted new bone formation surrounding the TiO_2 implants. This suggested that the kaempferol immobilized on TiO_2 was released in vivo and promoted osteogenic activity. These results are consistent with those of a previous report.[17] The kaempferol delivered by TiO_2 implants had bone formation effects similar to kaempferol delivered orally.[17] However, the in vivo results were not consistent with the in vitro results, as there was no significant difference between the two loading methods in this study. This result indicated that the release pattern of kaempferol was different in vivo and in vitro. Long-term investigations into the in vivo movements of labeled kaempferol are warranted. As far as we know, there are no published methods for the long-term, stable labeling of kaempferol in vivo. Further studies are required to determine the in vivo mobility of kaempferol. Osteoclasts were not observed around the TiO_2 implant. Kaempferol inhibits the receptor activator of NF-κB ligand-mediated osteoclastogenesis via the down-regulation of mitogen-activated protein kinase, c-Fos, and nuclear factor of activated T cells c1.[45] This result suggested that kaempferol released from a TiO_2 surface has an inhibitory role in bone loss by preventing osteoclast formation.

Finally, our in vitro results indicated that adsorption of kaempferol leads to the best cell responses in terms of cell attachment, proliferation, and osteogenic differentiation. As adsorbed kaempferol is simple and easy to prepare, safe, and cost effective, this method could be implemented for clinical trials.

Conclusion

Our results showed that adsorbed kaempferol on the surface of TiO_2 implants leads to good cell responses in terms of cell proliferation, ALPase activity, and osteogenic differentiation. In addition, adsorbed kaempferol on TiO_2 implants promotes bone morphogenesis during the early stages of osseointegration. Our results indicate that immobilizing kaempferol by adsorption and coprecipitation methods is an effective strategy for promoting bone regeneration around TiO_2 implants.

Acknowledgments

This work was supported in part by grants from the Japanese Ministry of Education, Culture, Sports, Science, and Technology (Kakenhi Kiban C, 17K11802 to Shuhei Tsuchiya; Kakenhi Kiban B, 16H05540 to Hideharu Hibi; and Kakenhi Kiban B, 00283408 to Kensuke Kuroda).

Disclosure

The authors report no conflicts of interest in this work.

References

1. Brånemark R, Brånemark PI, Rydevik B, Myers RR. Osseointegration in skeletal reconstruction and rehabilitation: a review. *J Rehabil Res Dev*. 2001;38(2):175–181.
2. Brånemark PI. Osseointegration and its experimental background. *J Prosthet Dent*. 1983;50(3):399–410.
3. Vandamme K, Holy X, Bensidhoum M, et al. In vivo molecular evidence of delayed titanium implant osseointegration in compromised bone. *Biomaterials*. 2011;32(14):3547–3554.
4. Xia L, Feng B, Wang P, et al. In vitro and in vivo studies of surface-structured implants for bone formation. *Int J Nanomedicine*. 2012;7:4873–4881.
5. Eom TG, Jeon GR, Jeong CM, et al. Experimental study of bone response to hydroxyapatite coating implants: bone-implant contact and removal torque test. *Oral Surg Oral Med Oral Pathol Oral Radiol*. 2012;114:411–418.
6. Morra M. Biomolecular modification of implant surfaces. *Expert Rev Med Devices*. 2007;4:361–372.
7. Sigurdsson TJ, Fu E, Tatakis DN, Rohrer MD, Wikesjo UM. Bone morphogenetic protein-2 for peri-implant bone regeneration and osseointegration. *Clin Oral Implants Res*. 1997;8:367–374.
8. Morra M, Cassinelli C, Cascardo G, et al. Surface engineering of titanium by collagen immobilization. Surface characterization and in vitro and in vivo studies. *Biomaterials*. 2003;24:4639–4654.
9. Gorbahn M, Klein MO, Lehnert M, et al. Promotion of osteogenic cell response using quasicovalent immobilized fibronectin on titanium surfaces: introduction of a novel biomimetic layer system. *J Oral Maxillofac Surg*. 2012;70:1827–1834.
10. Du C, Schneider GB, Zaharias R, et al. Apatite/amelogenin coating on titanium promotes osteogenic gene expression. *J Dent Res*. 2005;84:1070–1074.
11. Korn P, Schulz MC, Hintze V, et al. Chondroitin sulfate and sulfated hyaluronan-containing collagen coatings of titanium implants influence peri-implant bone formation in a minipig model. *J Biomed Mater Res A*. 2014;102(7):2334–2344.
12. Cao X, Yu WQ, Qiu J, Zhao YF, Zhang YL, Zhang FQ. RGD peptide immobilized on TiO2 nanotubes for increased bone marrow stromal cells adhesion and osteogenic gene expression. *J Mater Sci Mater Med*. 2012;23:527–536.
13. Song W, Song X, Yang C, et al. Chitosan/siRNA functionalized titanium surface via a layer-by-layer approach for in vitro sustained gene silencing and osteogenic promotion. *Int J Nanomedicine*. 2015;10:2335–2346.
14. Sharan K, Siddiqui JA, Swarnkar G, Maurya R, Chattopadhyay N. Role of phytochemicals in the prevention of menopausal bone loss: evidence from in vitro and in vivo, human interventional and pharma-cokinetic studies. *Curr Med Chem*. 2009;16:1138–1157.
15. Siddiqui JA, Sharan K, Swarnkar G, et al. Quercetin-6-C-β-D-glucopyranoside isolated from Ulmus wallichiana planchon is more potent than quercetin in inhibiting osteoclastogenesis and mitigating ovariectomy-induced bone loss in rats. *Menopause*. 2011;18:198–207.
16. Yang L, Takai H, Utsunomiya T, et al. Kaempferol stimulates bone sialoprotein gene transcription and new bone formation. *J Cell Biochem*. 2010;110(6):1342–1355.
17. Kumar A, Gupta GK, Khedgikar V, et al. In vivo efficacy studies of layer-by-layer nano-matrix bearing kaempferol for the conditions of osteoporosis: a study in ovariectomized rat model. *Eur J Pharm Biopharm*. 2012;82(3):508–517.

18. Miyake M, Arai N, Ushio S, Iwaki K, Ikeda M, Kurimoto M. Promoting effect of kaempferol on the differentiation and mineralization of murine pre-osteoblastic cell line MC3T3-E1. *Biosci Biotechnol Biochem*. 2003; 67(6):1199–1205.
19. Kumar A, Singh AK, Gautam AK, et al. Identification of kaempferol-regulated proteins in rat calvarial osteoblasts during mineralization by proteomics. *Proteomics*. 2010;10(9):1730–1739.
20. Choi EM. Kaempferol protects MC3T3-E1 cells through antioxidant effect and regulation of mitochondrial function. *Food Chem Toxicol*. 2011;49(8):1800–1805.
21. Rassi CM, Lieberherr M, Chaumaz G, Pointillart A, Cournot G. Modulation of osteoclastogenesis in porcine bone marrow cultures by quercetin and rutin. *Cell Tissue Res*. 2005;319:383–393.
22. Pang JL, Ricupero DA, Huang S, et al. Differential activity of kaempferol and quercetin in attenuating tumor necrosis factor receptor family signaling in bone cells. *Biochem Pharmacol*. 2006;71:818–826.
23. Prouillet C, Mazière JC, Mazière C, Wattel A, Brazier M, Kamel S. Stimulatory effect of naturally occurring flavonols quercetin and kaempferolon alkaline phosphatase activity in MG-63 human osteoblasts through ERK and estrogen receptor pathway. *Biochem Pharmacol*. 2004; 67:1307–1313.
24. Trivedi R, Kumar S, Kumar A, et al. Kaempferol has osteogenic effect in ovariectomized adult Sprague-Dawley rats. *Mol Cell Endocrinol*. 2008; 16:289(1–2):85–93.
25. Devi KP, Malar DS, Nabavi SF, et al. Kaempferol and inflammation: from chemistry to medicine. *Pharmacol Res*. 2015;99:1–10.
26. Verhoeyen ME, Bovy A, Collins G, et al. Increasing antioxidant levels in tomatoes through modification of the flavonoid biosynthetic pathway. *J Exp Bot*. 2002;53(377):2099–2106.
27. Calderón-Montaño JM, Burgos-Morón E, Pérez-Guerrero C, López-Lázaro M. A review on the dietary flavonoid kaempferol. *Mini Rev Med Chem*. 2011;11(4):298–344.
28. Jebahi S, Nsiri R, Boujbiha M, et al. The impact of orthopedic device associated with carbonated hydroxyapatite on the oxidative balance: experimental study of bone healing rabbit model. *Eur J Orthop Surg Traumatol*. 2013;23(7):759–766.
29. Schmidt-Bleek K, Kwee BJ, Mooney DJ, Duda GN. Boon and bane of inflammation in bone tissue regeneration and its link with angiogenesis. *Tissue Eng Part B Rev*. 2015;21(4):354–364.
30. Ripamonti U, Roden LC, Renton LF. Osteoinductive hydroxyapatite-coated titanium implants. *Biomaterials*. 2012;33(15):3813–3823.
31. Perets A, Baruch Y, Weisbuch F, Shoshany G, Neufeld G, Cohen S. Enhancing the vascularization of three-dimensional porous alginate scaffolds by incorporating controlled release basic fibroblast growth factor microspheres. *J Biomed Mater Res A*. 2003;65(4):489–497.
32. Chen C, Zhang SM, Lee IS. Immobilizing bioactive molecules onto titanium implants to improve osseointegration. *Surf Coat Technol*. 2013; 228 (Suppl 1):S312–S317.
33. Chen C, Li H, Kong X, Zhang SM, Lee IS. Immobilizing osteogenic growth peptide with and without fibronectin on a titanium surface: effects of loading methods on mesenchymal stem cell differentiation. *Int J Nanomedicine*. 2014;10:283–295.
34. Atsuta I, Yamaza T, Yoshinari M, et al. Changes in the distribution of laminin-5 during peri-implant epithelium formation after immediate titanium implantation in rats. *Biomaterials*. 2005;26(14):1751–1760.
35. Mohan L, Anandan C, Rajendran N. Drug release characteristics of quercetin-loaded TiO_2 nanotubes coated with chitosan. *Int J Biol Macromol*. 2016;93(Pt B):1633–1638.
36. Gregory CA, Gunn WG, Peister A, Prockop DJ. An Alizarin red-based assay of mineralization by adherent cells in culture: comparison with cetylpyridinium chloride extraction. *Anal Biochem*. 2004;329(1): 77–84.
37. Tsuchiya S, Hara K, Ikeno M, Okamoto Y, Hibi H, Ueda M. Rat bone marrow stromal cell-conditioned medium promotes early osseointegration of titanium implants. *Int J Oral Maxillofac Implants*. 2013;28(5): 1360–1369.
38. Yazaki Y, Oyane A, Sogo Y, Ito A, Yamazaki A, Tsurushima H. Control of gene transfer on a DNA-fibronectin-apatite composite layer by the incorporation of carbonate and fluoride ions. *Biomaterials*. 2011;32(21): 4896–4902.
39. Chen C, Qiu ZY, Zhang SM, Lee IS. Biomimetic fibronectin/mineral and osteogenic growth peptide/mineral composites synthesized on calcium phosphate thin films. *Chem Commun (Camb)*. 2011;47(39): 11056–11058.
40. Wu Z, Feng B, Weng J, Qu S, Wang J, Lu X. Biomimetic apatite coatings on titanium coprecipitated with cephradine and salviae miltlorrhizae. *J Biomed Mater Res B Appl Biomater*. 2008;84(2):486–492.
41. Barrère F, van der Valk CM, Dalmeijer RA, van Blitterswijk CA, de Groot K, Layrolle P. In vitro and in vivo degradation of biomimetic octacalcium phosphate and carbonate apatite coatings on titanium implants. *J Biomed Mater Res A*. 2003;64(2):378–387.
42. Yu X, Suárez-González D, Khalil AS, Murphy WL. How does the pathophysiological context influence delivery of bone growth factors? *Adv Drug Deliv Rev*. 2015;84:68–84.
43. Yoo SM, Cho SJ, Cho YY. Molecular targeting of ERKs/RSK2 signaling axis in cancer prevention. *J Cancer Prev*. 2015;20(3):165–171.
44. Cowles EA, DeRome ME, Pastizzo G, Brailey LL, Gronowicz GA. Mineralization and the expression of matrix proteins during in vivo bone development. *Calcif Tissue Int*. 1998;62(1):74–82.
45. Lee WS, Lee EG, Sung MS, Yoo WH. Kaempferol inhibits IL-1β-stimulated, RANKL-mediated osteoclastogenesis via downregulation of MAPKs, c-Fos, and NFATc. *Inflammation*. 2014;37(4): 1221–1230.